

MATHEMATICAL MODELLING OF WAVE-INDUCED NEARSHORE CIRCULATIONS

DONGHOON YOO¹ and BRIAN A. O'CONNOR²

The paper presents a mathematical model for describing wave climate and wave-induced nearshore circulations. The model accounts for current-depth refraction, diffraction, wave-induced currents, set-up and set-down, mixing processes and bottom friction effects on both waves and currents. The present model was tested against published experimental data on wave conditions within a model harbour and shown to give very good results for both wave and current fields. The importance of including processes such as advection, flooding and current-interaction in coastal models was demonstrated by comparing the numerical results without each process to the results from the complete scheme.

1. INTRODUCTION

Wave-induced nearshore circulations are the result of complex processes driven by gravity water waves. When waves approach either the shoreline or man-made coastal structures, processes of shoaling, refraction, diffraction, dissipation and wave-current interaction occur. When waves propagate closer to the shoreline or diffract behind a breakwater, nearshore currents are produced by the excess momentum flux of the waves (radiation stresses). The nearshore currents are then modified by bottom friction and mixing processes, particularly in the surf zone. An additional effect produced by the presence of the waves is a change in mean water level, called set-up and set-down.

The last two decades have seen tremendous developments in the study of nearshore circulations induced by waves, with the establishment of various wave models and the use of more realistic closure models of bottom friction and mixing processes. Although recent numerical models have enabled a mathematical formulation of many of the nearshore processes to be made, a comprehensive model, which is able to describe all engineering situations, has yet to be developed. The model presented in the present paper is an attempt by the authors to improve the engineering modelling of complex nearshore processes.

In the present paper, an attempt is made to refine the classical ray model including the effects of diffraction and current-interaction, see also Yoo and O'Connor⁽¹³⁾. Thus, the new ray model is able to deal with large or small scale areas involving caustic zones and/or

¹Research Associate, Dept. of Civil Eng., University of Liverpool.

²Professor, Dept. of Civil Eng., University of Liverpool, P.O. Box 147, Liverpool, L69 3BX, U.K.

diffraction in the lee of coastal structures. The wave field is defined at regular grid points, and hence any interpolation procedure often required for ray tracking method is avoided.

2. KINEMATICS OF REFRACTIVE AND DIFFRACTIVE WAVES IN SLOWLY VARYING CURRENT FIELD

For a plane wave, the wave number vector K_i and the wave frequency σ are given, respectively, by the spatial gradient and the time derivative of the phase function D . The local values of the slowly varying wave number vector and the frequency of the nearly plane wave may also be described by the same definitions, and the kinematic conservation is obtained from the definitions:-

$$\frac{\partial K_i}{\partial t} + \frac{\partial \sigma}{\partial x_i} = 0 \quad (1)$$

along with the zero-vorticity equation:-

$$\frac{\partial K_i}{\partial x_j} = \frac{\partial K_j}{\partial x_i} \quad (2)$$

where t is time, x is the cartesian coordinate and $i, j=1, 2$ as in conventional tensor notation.

When the waves propagate on a current we also have the Doppler relation:-

$$\sigma = \sigma_0 + K_i U_i \quad (3)$$

where σ is the apparent or observed angular frequency, σ_0 is the intrinsic or Doppler-shifted angular frequency and U is the current velocity.

Waves generally appear to be propagating on still water in the moving frame of reference. All the relevant equations for the wave field are valid, therefore, on the moving frame of reference and the dispersion relation can be used in the form:-

$$\sigma_0^2 = gk \tanh kd \quad (4)$$

where g is the acceleration due to gravity, d is the water depth and k is the separation factor, which is the same as the wave number K (eiconal) for non-diffractive waves.

Battjes⁽¹⁾ discovered that the wave number K is not eiconal to k when diffraction occurs and produced the following relation:-

$$K^2 = k^2 + \delta^* = (1 + \delta)k^2 \quad (5)$$

where

$$\delta^* = \frac{1}{a} \frac{\partial^2 a}{\partial x_i^2} \quad (6)$$

$\delta = \delta^*/k^2$ and a is the wave amplitude. The wave number vector is not affected by a translation of coordinates. Thus equation (5) will be valid without modification for waves on a current.

It is then realised that

$$\sigma = \sigma(\sigma_0(k, d), K_i(k, \delta^*), U_i) \quad (7)$$

where the variables in the brackets are independent of each other. Differentiating equation (7) with respect to x_i using the chain rule and inserting it into equation (1) with the zero vorticity equation (2) produces the kinematic conservation equation for the wave number vector K_i :-

$$\frac{\partial K_i}{\partial t} + (R_j + U_j) \frac{\partial K_i}{\partial x_j} + S \frac{\partial d}{\partial x_i} + K_j \frac{\partial U_j}{\partial x_i} - \frac{R}{2ka} \frac{\partial^3 a}{\partial x_i \partial x_j^2} = 0 \quad (8)$$

where R_j are the intrinsic group velocity components given by

$$R_j = \frac{K_j}{k} R \quad (9)$$

$$R = \frac{1}{2} (1 + G) \frac{\sigma_\theta}{k} \quad (10)$$

$$S = \frac{G}{2} \frac{\sigma_\theta}{d} \quad (11)$$

$$G = \frac{2kd}{\sinh 2kd} \quad (12)$$

Here the second order derivatives of amplitude curvature are ignored. The last term of equation (8) expresses the diffraction effect on the transformation of kinematic wave properties. It further corrects the number of waves per unit length, depending on the gradient of amplitude curvature. Existing ray theories lack this term, and hence such methods fail to ensure kinematic conservation when diffraction occurs.

3. DYNAMICS OF WAVES AND TURBULENT CURRENTS

The major equations governing the dynamic motion of waves and turbulent currents derive from the conservation equations of motion. The wave-period and depth-averaged forms of the governing equations are as follows (see Yoo⁽¹²⁾ for details):-

$$\frac{\partial \eta}{\partial t} + \frac{\partial}{\partial x_i} (d U_i) = 0 \quad (13)$$

$$\frac{\partial U_i}{\partial t} + U_j \frac{\partial U_i}{\partial x_j} + \frac{1}{\rho d} \frac{\partial S_{ij}}{\partial x_j} + g \frac{\partial \eta}{\partial x_i} + \frac{|U|}{d} C^U U_i U_i = \frac{\partial}{\partial x_j} \epsilon_j \frac{\partial U_i}{\partial x_j} \quad (14)$$

$$\frac{\partial a}{\partial t} + \frac{1}{2a} \frac{\partial}{\partial x_i} \{ (R_i + U_i) a^2 \} + \frac{S_{ij}}{\rho g a} \frac{\partial U_j}{\partial x_i} + C^a a^2 = 0 \quad (15)$$

where η is the wave-period-average surface elevation, ρ is the water density, ϵ_j are eddy mixing coefficients, C^U is the bottom friction coefficients associated with U_i , C^a is the bottom friction coefficient associated with a , and S_{ij} are the radiation stresses given by

$$S_{ij} = \left\langle \int_{-h}^{\zeta} (\rho \tilde{u}_i \tilde{u}_j + p \delta_{ij}) dz - \int_{-h}^{\eta} p_0 \delta_{ij} dz \right\rangle \quad (16)$$

where ζ is the instantaneous surface elevation, h is the bottom elevation, \tilde{u} is the wave particle velocity, p is the dynamic pressure, p_0 is the hydrostatic pressure and δ_{ij} is the Kronecker delta.

If it is assumed that the wave field is independent of the turbulent current field in such a way that any input or output of wave energy due to turbulent motion is made in an indirect way, the wave motion may be described by a potential formulation.

If we define the wave velocity potential by the equation:-

$$\tilde{u}_\alpha = - \frac{\partial \varphi}{\partial x_\alpha} \quad (17)$$

where $\alpha = 1, 2, 3$, from the Laplace and Bernoulli equations for the linear sinusoidal waves we have:-

$$\varphi = \frac{ga}{\sigma_0} \frac{\cosh k(h+z)}{\cosh kd} \cos D \quad (18)$$

where z is the water elevation. Substituting Equation (17) with Equation (18) into Equation (16) yields:-

$$S_{ij} = \frac{1}{2} \left\{ (1 + \delta)(1 + G) \frac{K_i}{K} \frac{K_j}{K} + G \delta_{ij} \right\} \left(\frac{1}{2} \rho g a^2 \right) \quad (19)$$

Equation (19) is the general expression for the radiation stresses of refractive and diffractive waves.

The four depth and wave-period averaged equations (8, 13, 14 and 15) form the basis of the present model and describe the wave and current fields in interacted flow. Equations (13) and (14) describe the current field, while equation (15) describes the wave field, when considered along with equation (8). It is also clear from the above equations that any solution of the proposed model requires proper estimation of the coefficients C^U , C^a and ϵ_j . In the surf zone, wave heights are eventually controlled by breaking, and a breaking criterion has commonly been used to limit wave height. In the present investigation, improved closure sub-models for evaluating such parameters are used. They are outlined in the following section.

4. CLOSURE SUBMODELS

MIXING PROCESS

Though many researchers seem to have realised that the mixing process in the surf zone should be related to the amount of wave energy dissipated by breaking, only Battjes⁽²⁾ derived the velocity scale of turbulence from any sort of parameter directly related to the wave breaking. He found the cube root of the energy dissipation rate to be a proper measure of the velocity scale for turbulent eddy viscosity. He also suggested that the characteristic size of eddies would be primarily restricted by their vertical extent rather than their horizontal extent. This fact is well known in the field of river engineering. Many experimental and field measurements have indicated the strong depth-dependency of both horizontal and vertical eddy viscosity (see Fisher, et al. ⁽⁵⁾).

Since the present wave amplitude equation (15) is of a transient form, the dissipation rate induced by wave breaking can easily be evaluated by checking to see if breaking has occurred, using a breaking criterion. If the wave amplitude given by equation (15) exceeds the breaking limit, the excess energy is considered to contribute to mixing processes. Otherwise, mixing processes would not be directly influenced by wave breaking.

The cube root of the energy dissipation rate, divided by fluid density, might be called the 'dissipation speed', since the square root of the bottom shear stress, divided by fluid density, is called the '(bottom) frictional velocity'. This concept is useful for considering the eddy motion of pure oscillatory flow or combined wave and current flow. Since significant amount of eddy motion is expected from bottom friction, even in the surf zone, a velocity scale for the eddy viscosity should also be related to the bottom friction. However, while a frictional velocity has been successfully used for modelling mixing process in uni-directional channel flows, it is of no use for oscillatory flow since the wave-period-average bottom friction of oscillatory flow vanishes.

In the present surf zone studies, the contribution of the bottom friction on the eddy motion is taken into account by regarding the combined breaking and frictional dissipation speed as the proposed velocity scale for the eddy viscosity. The inclusion of the bottom friction improves the Battjes' eddy viscosity model, which displays a sharp discontinuity at the breaking point.

The turbulent motion is also assumed to be anisotropic, and hence some allowance for directional preference is made in the model when describing the eddy viscosity. It has been assumed that the eddy viscosity has an ellipsoid form, of which the semi-major axes is determined by 60% of the total energy dissipation and the minor axes by 20%. The details are found in the recent work of Yoo⁽¹²⁾.

BOTTOM FRICTION

Bottom friction has been recognised as one of the most important factors balancing the forces driven by radiation stresses in the nearshore circulation system. Due to this recognition, several numerical modellers have made efforts to evaluate more precisely the period-average bottom friction of the combined flow. However, in their approaches the friction factor was kept constant over the whole domain and its value seems to have been determined somewhat arbitrarily by the modeller's own personal view of the problem.

Fortunately, several detailed models now exist for evaluating the bottom shear stress of combined interacting wave and current flows. However, the majority of these models are too complex or involve time-consuming computer methods which are unsuitable for use in an engineering model of coastal circulations where many calculations have to be performed at a large number of grid points. The present authors have, therefore, taken one of the simpler "detailed models", that due to Bijker⁽⁴⁾, and have modified it to include the effects of the reduction in mean current speed due to the presence of the waves. The modification also enabled expressions to be produced for the total energy dissipation rate and enhanced wave energy dissipation rate and the coefficients C^U and C^a .

The improved Bijker approach, see Yoo⁽¹²⁾ and O'Connor and Yoo⁽⁹⁾ for further details, was tested against results from other detailed models. It was shown to be as good as the more complex models and to be better than the existing simpler models but to take up little computation time. It was therefore adopted for the present model.

BREAKING CRITERION

The transformation of waves in the surf zone is eventually controlled or limited by wave breaking which results from the loss of stability of wave formation and in turn provides a major contribution to surf zone mixing processes. It has been common practice to describe the breaking process by a simple criterion which allows the wave growth only up to a certain limit.

Miche's criterion⁽⁸⁾ has been widely used for numerical computation due to its mathematical reliability and broad coverage from deep to shallow water. In the late 1960's it was realised from experimental evidence that beach slope influenced the breaking mechanism and criterion. To include the slope effect, Miche's criterion was reworked by Battjes & Janssen⁽³⁾ as follows:-

$$(Ka)_b = \frac{\pi}{7} \tanh(q Kd)_b \quad (20)$$

where $q_b = (7/\pi) \gamma_b$ and γ_b is the ratio of wave amplitude to the water depth at the breaking point $(a/d)_b$. In this formulation, they also matched equation (20) with the breaking criterion for solitary waves in very shallow water, i.e., when $kd \rightarrow 0$ to find the value for q_b .

The factor q_b or γ_b may also be evaluated by empirical equations related to the bed slope. However, the existing relations do not take into account the current-interaction effect, which can be significant in the nearshore circulation system. Based on a theoretical reasoning, a new surf zone parameter β , applicable to the current-interacted situation, was developed by the authors. The parameter β is the relative intensity of the residual kinematic group velocity to the depth-mean energy propagation velocity. In the combined flow we may replace them by the absolute velocities, i.e.

$$\beta = \frac{R - P}{R + U_w} \quad (21)$$

where R is the relative kinematic group velocity, P is the depth-mean energy propagation velocity and U_w is the current velocity in the wave direction. Using the new parameter, a number of experimental data sets were examined and the following relation found (Yoo⁽¹²⁾):-

$$q_b = 0.8 + \tanh(90\beta) \quad (22)$$

Equation (21) also expresses that waves are liable to be more easily broken when they encounter an opposing current as the surf parameter reaches a higher value than when they propagate with a following current.

5. NUMERICAL MODELLING

The combined wave and current flow in coastal areas has been described by the set of Eulerian conservation equations, that is, equations (8) and (15) for the wave field and equations (13) and (14) for the current field. The bottom friction coefficients C^U and C^a and the mixing coefficients ϵ_j are defined using closure models, while the wave amplitude is given by equation (15), unless the breaking criterion of equation (20) shows a limited wave height at which point excess wave energy is transferred to mixing processes.

Due to several complicated non-linear terms in the equations, the solution of the system is best achieved by using numerical techniques. Finite difference explicit schemes are employed for solving both wave and current equations, since the full interaction between waves and currents is taken into account. It is here emphasised that the long and complex procedure of solving large number of simultaneous equations at each time step negates the large time step allowed by implicit schemes and drastically reduces the efficiency of implicit methods. Therefore, explicit schemes are chosen for the present work.

The angled derivative explicit (ADE) scheme, which was introduced by Flather & Heaps⁽⁸⁾ for tide modelling, is used for solving the current momentum equations, while an upstream differencing scheme is used for solving the wave equations. Since waves are assumed to be progressive, the 'upstream' differencing scheme, which controls the direction of differencing by the direction of the progressive motion, was found to be an excellent choice for the wave equations (see Yoo⁽¹²⁾ and Yoo & O'Connor⁽¹³⁾ for details).

The solutions of finite difference forms of the governing equations are obtained by providing initial and boundary conditions. Tests with the model showed that the best arrangement was a 'cold start' for the current field with a flat water surface and zero current velocity everywhere and a 'hot start' for the wave field, that is, the wave variables over the modelled area were set to be the same as the inflow boundary values. Tests also showed that the initial errors were quickly damped down particularly in the surf zone, by imposing a breaking criterion which prevents excessive build-up of wave energy. No-flow condition was applied to the inflow boundary at the offshore end as well as to the land boundary.

In order to cope with situations involving the 'wetting' and 'drying' of computational grids, the Flather and Heaps' scheme⁽⁶⁾ is employed in the present model, which tests the wet condition at each velocity point instead of each elevation point. It can allow the flooding from any direction and generally ensures mass continuity during a transition period from wet to dry or dry to wet. Unrealistically high velocities were found on steep slopes when the condition changed from wet to dry. This was improved by imposing a sensible depth, below which the flow velocity was put to zero, see Yoo⁽¹²⁾.

6. MODEL APPLICATION

The present model has been tested against several well-controlled experiments with satisfactory results (Yoo⁽¹²⁾). The present paper presents a set of results obtained on a model breakwater study. The experiments were conducted by Gourlay⁽⁷⁾ to study the nearshore circulation produced behind a semi-detached breakwater normal to the direction of wave approach (see Fig. 4 of Gourlay⁽⁷⁾). The beach behind the breakwater was formed of concrete. In the sheltered area behind the breakwater, it was curved with a constant radius centred on the breakwater tip. The water depth offshore of the beach was maintained at 20 cm throughout the tests. The inflow wave conditions were $a = 45.5$ mm and $T = 1.5$ seconds with waves propagating normal to the breakwater.

The investigation area was resolved by finite difference meshes of $\Delta x = 0.185$ m and $\Delta y = 0.2075$ m with 41 meshes in the x direction and 34 meshes in the y direction (see Fig. 1). The left-hand side of the training wall in front of the breakwater was not included in the computation domain and the inflow wave condition was imposed along the line at the offshore end of the training wall. The time step chosen was 0.005 seconds to ensure computational stability.

A value of 0.001m was chosen for the effective roughness height of the concrete in the model. Several trials with the model showed that the dimensionless mixing coefficients $M_b = 2.0$ and $M_f = 4.0$ gave the best solution for the present case. The value of $M_b = 2.0$ is similar to that ($M_b = 3.0$) found by Visser⁽¹¹⁾ using experimental results for a uniform beach.

Fig. 2 shows the time variations of the wave amplitude, current velocity and mean surface elevation at the inshore points A and B (see Fig. 1). While the mean surface elevation still substantially

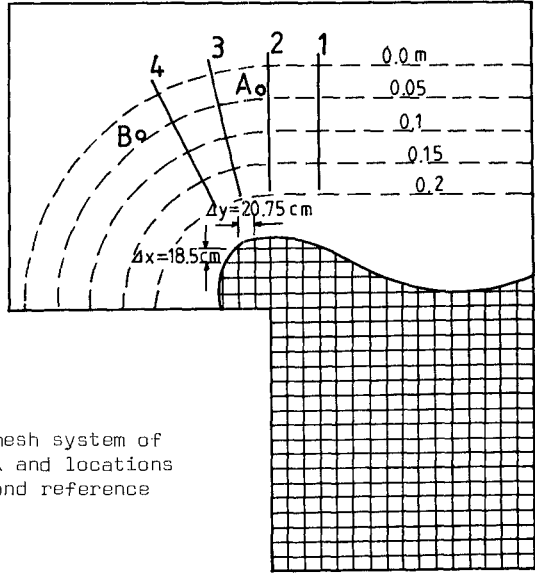


Fig. 1 Finite difference mesh system of Gourlay's wave tank and locations of cross-sections and reference points

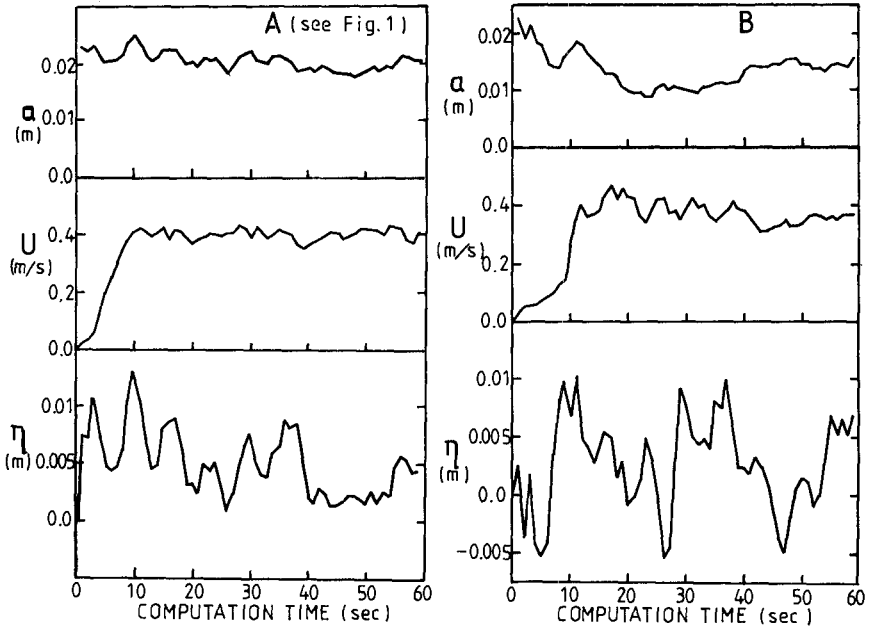


Fig. 2 Time variations of wave amplitude, current velocity and mean surface elevation at locations A and B.

oscillates up to 60 seconds, both wave amplitude and current velocity soon fully develop within a short period. It is interesting to note that at location B the wave amplitude gradually decreases below 0.01m up to 24 seconds, then slowly increases over 0.013m up to 40 seconds and finally remains relatively constant during the rest of the computation period. This changing history of the wave amplitude is certainly caused by the current interaction effects, which seem to alter the wave environment significantly over the whole area.

From Fig. 2, it is believed that the steady state is reached roughly at around 40 seconds. It was, therefore, decided that the result at 50 seconds was likely to be the final solution for the flow field in the present case. The results at time 50 seconds are shown in succeeding figures; wave height distribution in Fig. 3 and wave-induced currents in Fig. 4. The computed results are compared with the experimental data in plan and detailed comparison of the current values is made on several cross sections (refer to Fig. 1 for the details of the location of the cross sections). The agreement between the model and the experiment results is seen to be very good overall.

The computed wave height distribution is seen to be very similar to the experimental one (see Fig. 3). Some minor deviations are found in the middle of the right-hand side of the tank and in the left-hand corner behind the breakwater. Higher values at the left-hand corner in the lee of the breakwater seem to be due to reflection from the beach, while lower values in the middle of the right-hand side may be caused by the non-linear effect of wave transformation near the breaker zone.

The computed current pattern agrees quite well with the experimental one, both qualitatively and quantitatively (see Fig. 4). The computed main gyre behind the breakwater is located at a similar position to the experimental one, being located about 0.5m further inside the breakwater, while even the small eddy motion at the left-hand corner behind the breakwater is well represented by the present model. The detailed comparison of the currents on several cross sections shows the quite good agreement of the model results with the experimental ones in both offshore and inshore regions. In offshore regions, the model slightly over-estimates the current velocity, while inside the surf zone slightly under-estimates it. But the difference is considered acceptable, in view of likely errors in the measurement of conditions in the physical model and the limitation of grid resolution.

The model was finally employed for demonstrating the significance of the role of each term; advection, current-interaction and flooding. This can be best achieved by producing the computational results excluding each term and comparing them with the results from the experiments or the complete scheme. The computation results at 50 seconds are shown in Fig. 5, together with the results from the complete scheme. Problems were found when excluding the advection terms of the momentum equation. The flow developed so rapidly near the coastline that eventually the whole system became unstable at a

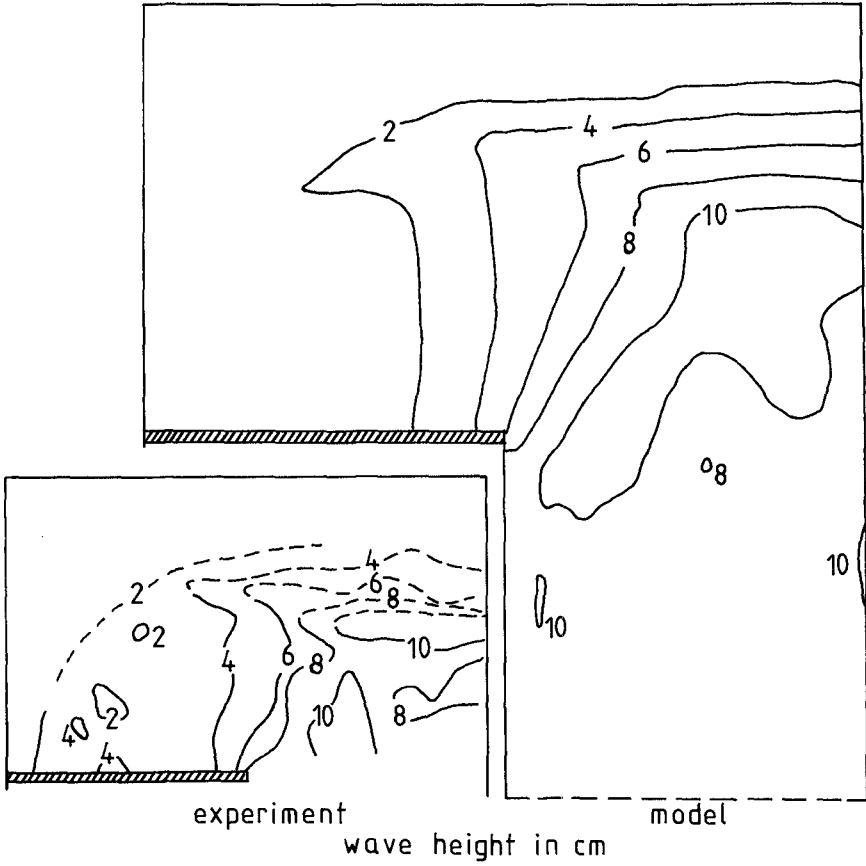


Fig. 3 Comparison of wave height between Gourlay's experiment and the present model.

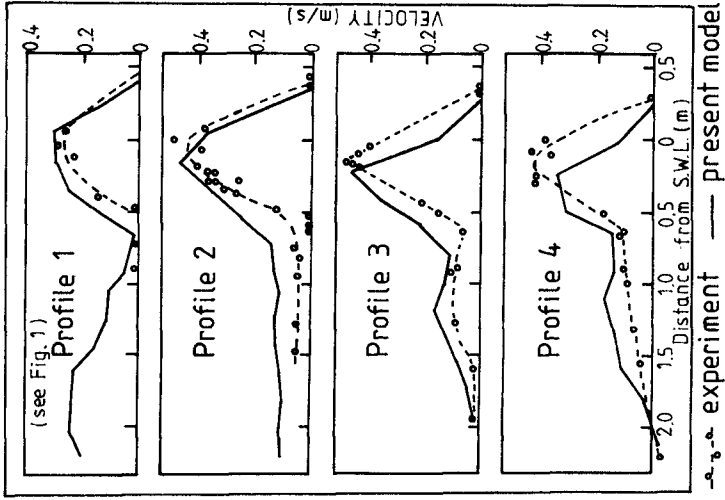
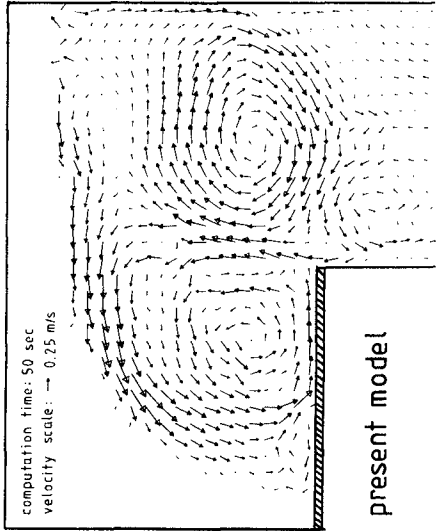
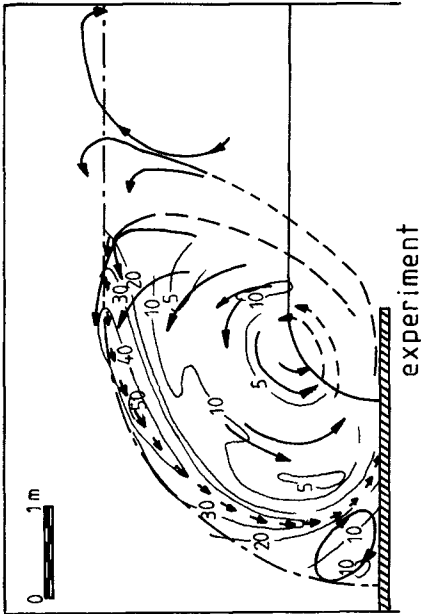
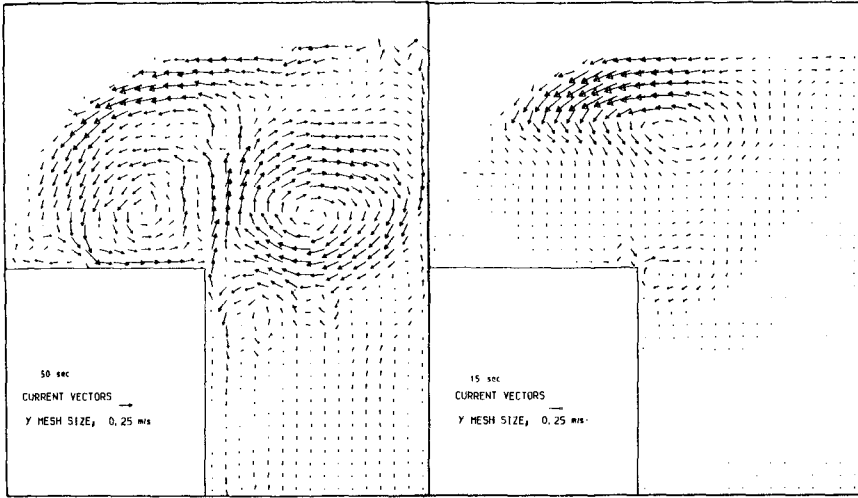


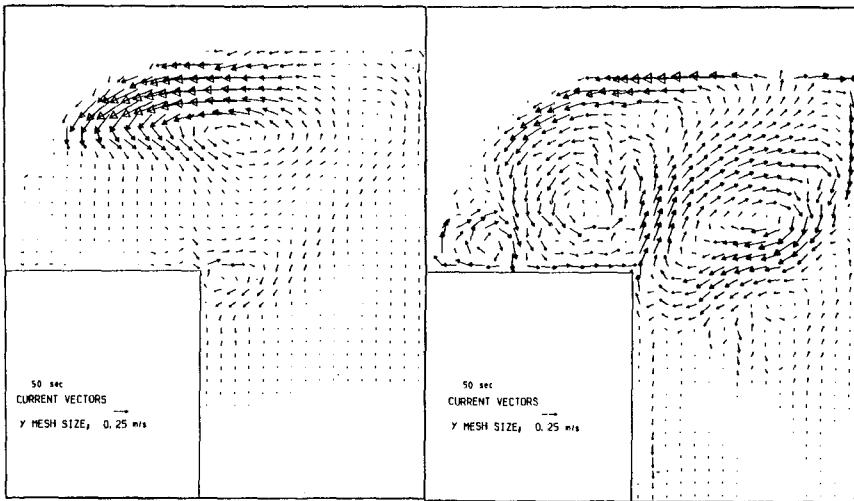
Fig. 4 Comparison of current velocity between Gourley's experiment and the present model





(1) complete

(2) no-advection



(3) no-current-interaction

(4) no-flooding

Fig. 5 Velocity distributions of wave-induced currents from different versions of the present model

run time of about 18 seconds. Therefore, the intermediate result at 15 seconds after the start of the computation is presented for the no-advection case.

Both schemes of no-advection and no-current-interaction are incapable of representing the small eddy motion at the left-hand corner behind the breakwater, while the centre of the main gyre is located a considerable distance from the experimental one. A totally wrong current pattern is thus given by the no-advection and no-current-interaction schemes. By contrast, the no-flooding scheme seems to have described the current pattern nearly as well as the complete interaction one. However, it generally over-estimates the current velocity particularly near the coast; the maximum velocity of the main gyre being predicted at over 65 cm/sec compared with about 50 cm/sec from the experiment, and the maximum velocity of the small gyre at over 25 cm/sec compared with about 10 cm/sec in the experiment. Therefore, if flooding is not included in the model, it is clear that incorrect answers will be obtained for both elevation and current velocity and, indirectly, for mixing coefficients.

7. CONCLUSION

The present work has been concerned with the development of an engineering computer model for evaluating both wave and current fields, particularly when they interact with each other as in the surf zone. The present wave model is fully based on ray theory, which has been extensively used in evaluating wave condition in field situations. The major deficit of existing ray models is that they are incapable of handling caustic or diffractive waves and hence the results are of limited use in areas with complex topography.

The present paper has shown how diffraction effects may be taken into account together with current-interaction effects. The authors' early works^(1,2,3) proved the capability of the present ray model for handling caustic waves, while the present paper demonstrates the model's ability for evaluating the wave-current flow fields in breakwater situation while fully accounting for diffraction and the interaction between waves and current. The model is shown to give very good results for both wave and current fields.

Comparison of model and laboratory tests illustrate the effects of current interaction on wave transformation as well as the current field itself; non-linear advective accelerations on momentum transfer; and flooding of flat zones due to set-up. When any one of the above processes is excluded, the current pattern is shown to be strikingly different from the experimental result or the complete, computer model result.

8. ACKNOWLEDGEMENT

This research is supported by the Science and Engineering Research Council through its Marine Technology Directorate and Marinetech North West, U.K.

9. REFERENCES

1. Battjes, J.A., 'Refraction of Water Waves', Journal of Waterways, and Harbors Division, ASCE, Vol. 94, WW4, 1968, pp. 437-451.
2. Battjes, J.A., 'Turbulence in the Surf Zone', Proceedings of the Modelling Techniques, ASCE, 1975, pp. 1050-1061.
3. Battjes, J.A. and Janssen, J.P.F.M., 'Energy Loss and Set-up due to Breaking of Random Waves', Proceedings of the 16th Conference of Coastal Engineering, ASCE, 1978, pp. 569-589.
4. Bijker, E.W., 'The Increase of Bed Shear in a Current due to Wave Motion', Proceedings of the 10th International Conference on Coastal Engineering, ASCE, 1967, pp. 746-765.
5. Fisher, H.B., List, E.J., Koh, R.C.Y., Imberger, J. and Brooks, N.H., 'Mixing in Inland and Coastal Waters, Academic Press, 1979, pp. 104-112.
6. Flather, R.A. and Heaps, N.S., 'Tidal Computations for Morecambe Bay', Geophysical Journal of Royal Astronomical Society, Vol. 42, 1976, pp. 489-517.
7. Gourlay, M.R., 'Wave Set-Up and Wave Generated Currents in the Lee of a Breakwater or Headland', Proceedings of the 14th International Conference on Coastal Engineering, ASCE, 1974, pp. 1976-1995.
8. Miche, M., 'Mouvements ondulatoires de la mer en profondeur constant ou décroissante', Annales des Ponts et Chaussées, 1944.
9. O'Connor, B.A. and Yoo, D., 'Mean Bed Friction of Combined Wave and Current Flow', Coastal Engineering, (submitted).
10. Swart, D.H., 'Offshore Sediment Transport and Equilibrium Beach Profiles', Delft Hydraulic Laboratory, Publication 131, 1974.
11. Visser, P.J., 'Uniform Longshore Current Measurements and Calculations', Proceedings of the 19th International Conference on Coastal Engineering, ASCE, 1984, pp. 2192-2207.
12. Yoo, D., 'Mathematical Modelling of Wave-Current Interacted Flow in Shallow Waters', Ph.D. Thesis, University of Manchester, 1986.
13. Yoo, D. and O'Connor, B.A., 'Ray Model for Caustic Gravity Waves', Proceedings of the 5th Congress of Asian and Pacific Division, International Association of Hydraulic Research, Vol. 3, 1986, pp. 1-13.